Process Modeling and Device-Package Simulation for Optimization of MEMS Gyroscopes

Xiaolin Chen, Wei Cui and Wei Xue

Washington State University Vancouver, {chenx,wei_cui,wxue}@vancouver.wsu.edu

ABSTRACT

Typical MEMS simulation mainly focuses on device performance without considering fabrication capabilities and packaging integratibility. This practice often leads to an inefficient product development cycle and increases the cost. This paper presents an integrated simulation workflow that incorporates the modeling of fabrication process, design analysis and packaging through a case study of a MEMS tuning-fork gyroscope using Coventorware. The device design is automatically generated based on mask layout and fabrication process restrictions. Design verification is performed both at the device-level for detailed analysis and at the system-level for behavior characterization. The effect of package deformation due to the thermal stress on the MEMS device is evaluated and discussed. The multi-level simulation presented here is proved to be an efficient way to accelerate the design process and improve the device performance, and can be used effectively to optimize the gyroscope system.

1. INTRODUCTION

Micromachined inertial sensors, including accelerometers and gyroscopes, are one of the most important devices in microelectro-mechanical systems (MEMS) [1]. They are among the most commercialized devices with the market size of billions of dollars [2]. In particular, MEMS gyroscopes have attracted a lot of attention in recent years. Unlike accelerometers, which detect the linear motion, gyroscopes measure the angular velocity of the system in the inertial reference frame. By integrating the measured angular velocity with the known initial conditions, the orientation of the system can be obtained and updated in real time [3]. A number of vibratory gyroscopes have been developed based on various designs such as oscillating beams [4, 5], vibrating shells [6] and tuning forks [7, 8, 9]. They are finding increasing applications in aircraft navigation systems, automobile air bags, video-camera stabilization systems, inertial mouse for computers, game remotes, etc. [10].

The high demands for micromachined inertial sensors require the mass production of devices with high performance, low cost, ease of fabrication, efficient packaging, and the ability to integrate the devices with control circuits. Ideally, all the aspects of MEMS design need to be carefully considered ranging from material selection, structure layout, fabrication capabilities, to packaging integratibility. To keep up with the design complexity, MEMS researchers are relying more on MEMS simulation tools so that the device performance can be verified and optimized prior to any prototyping or system integration. Nevertheless, typical MEMS simulation that involves both structural and circuitry modeling are often performed using general-purpose tools that traditionally exist in two different engineering fields. Design communication is hard to achieve with these discipline-specific packages.

Modeling results from different physical domains as well as results at different level of abstraction cannot be easily related or integrated. Design verification and optimization remain a challenge for these highly integrated miniaturized devices.

By using a tuning-fork gyroscope as an example, this paper presents a case study of multi-level simulation and optimization for a MEMS design with CoventorWare. The MEMS sensor is created based on process modeling following strict fabrication constraints. Modal and frequency response analyses are carried out using finite element and reduced-order modeling techniques to assess the device behaviors. Design optimizations are discussed in depth. With the optimized device, sensitivity analysis, Monte Carlo simulation and packaging analysis are further performed. Results show that the multi-level simulation scheme presented in this paper can be an effective way of optimizing MEMS to significantly reduce post-design fabrication cost and improve device performance.

2. OPERATION PRINCIPLE OF THE TUNNING-FORK GYROSCOPE

The motion detection of MEMS inertial sensors is based on the conversion from mechanical movement caused by the inertial force to the output electronic signals. The performance of the sensor relies heavily on the accuracy of the motion detection mechanism. Therefore, valid operation principles and proper designs are critical factors to determine the sensor performance. For most reported tuning-fork gyroscopes, the measurement of the angular velocity is based on the Coriolis effect [11]. This effect simplifies the fabrication process by using vibrating structures instead of rotating parts.
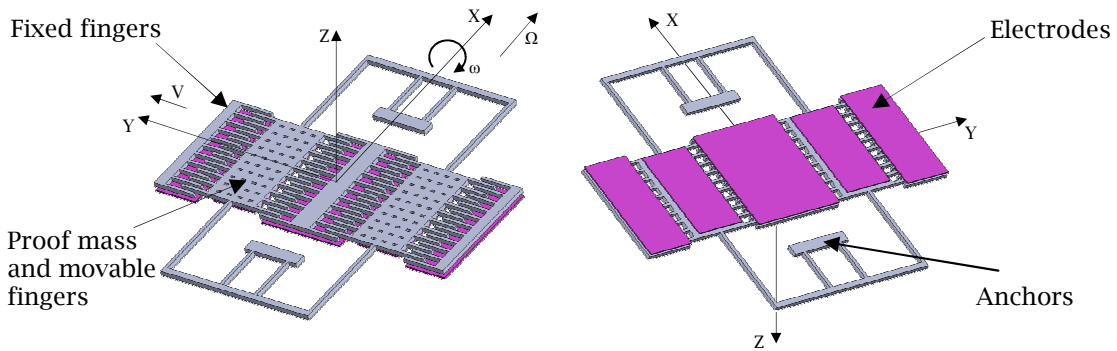

Fig. 1: The structure of a tuning-fork gyroscope.

The typical structure of a tuning-fork gyroscope is shown in Fig. 1 [9]. The gyroscope consists of two anchors, four suspension beams, two movable parts, four sets of fixed comb fingers, and electrodes on the backside. The corresponding coordinate system is also illustrated in the figure with the XY plane as the plate plane. The movable parts, including proof mass and attached comb fingers, vibrate with a velocity V along the Y-axis. The motion in this direction is driven into resonance by the comb drives. Once the sensor begins to rotate at a rate of ω around the X-axis, the entire device is subject to angular acceleration. The angular acceleration vector Ω has the same magnitude as ω with a direction along the X-axis. The fixed parts, including the anchors and the fixed fingers, move at the same rotation rate while the suspended proof mass is subject to a force induced by the acceleration. The force and the acceleration are called Coriolis force and Coriolis acceleration, respectively [12, 13]. The Coriolis acceleration is expressed by $2\Omega \times V$ and it is perpendicular to the plate plane. As a result, the Coriolis force moves the proof mass vertically out of the plate plane. Because the plate and electrodes underneath form a parallel-plate capacitor, the gap change between the plate and the substrate is converted to the capacitance change, which can be easily detected by the control circuit.

Based on the Coriolis effect, the tuning-fork gyroscope needs to work in two operation modes: driving mode along the Y-axis and sensing mode along the Z-axis. To achieve the maximum out-of-plane deflection, the resonant frequencies of the proof mass in the Y and Z directions must be closely matched. Therefore, the frequency response of the structure must be carefully designed to maximize the coupling between the driving mode and the sensing mode.

3. PROCESS MODELING

Most traditional MEMS modeling tools focus on the structural behavior without considering the device fabrication process [14, 15]. Ignoring the fabrication capabilities often leads to an inefficient product development cycle and an increased cost. Using CoventorWare, we can create a design model of the tuning-fork gyroscope taking the manufacturability into consideration. Besides the abilities to create 2D layout and 3D structures, the software package allows us to model the realistic deposition and etching steps in the microfabrication process.

Fig. 2 illustrates the 2D layout of the gyroscope with the dimensions of the initial design labeled. The gap between the proof mass and the electrodes underneath is 3 μm. The small gap increases the damping coefficient of the proof mass due to the squeeze-film effect. Therefore, the proof mass is perforated with etched holes to reduce the out-of-plane damping effect.
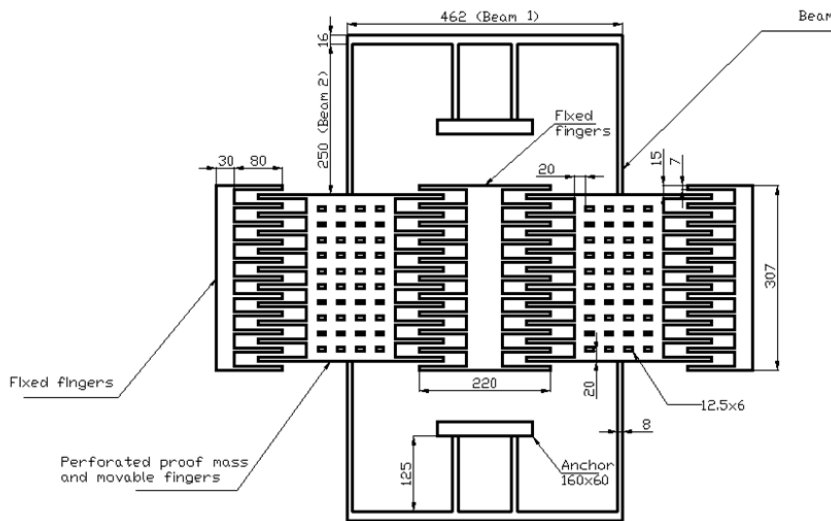

Fig. 2: The layout of the tuning-fork gyroscope (Unit: μm).

Step No.	Process Name	Material	Thickness (μm)
1	Substrate	Silicon	20
2	Deposit Insulator	Silicon Nitride	0.5
3	Deposit to Create Electrodes	Polysilicon	0.5
4	Deposit Sacrifice layer	Polymide	3
5	Etch Anchor Positions	Polymide	3
6	Conformal Deposit for Gyroscope	Silicon	20
7	Etch to Create Gyroscope	Silicon	20
8	Etch to Create Perforations	Silicon	20
9	Remove Sacrifice Layer	Polymide	3

Tab. 1: Fabrication steps for the gyroscope.

Tab. 1 summarizes the fabrication steps, material selections and the corresponding film thicknesses. Fig. 3 illustrates the key steps of the process modeling. A silicon wafer is used as the starting material (Fig. 3(a)). A layer of Si_3N_4 is deposited on the substrate as the insulation film. Next, a layer of

polysilicon is deposited on the surface and patterned as electrodes by lithography (Fig. 3(b)). A polymide film is coated on the substrate as the sacrificial material. After opening windows for the anchors and fixed fingers by lithography and selective etching (Fig. 3(c)), the entire device surface is covered by a thick layer of silicon which is used as the structural material for both the movable parts and fixed structures (Fig. 3(d)). Next, the silicon layer is selectively etched to generate the structures and perforations on the proof mass (Fig. 3(e)). The final step is to remove the sacrificial layer and release the movable structures (Fig. 3(f)).
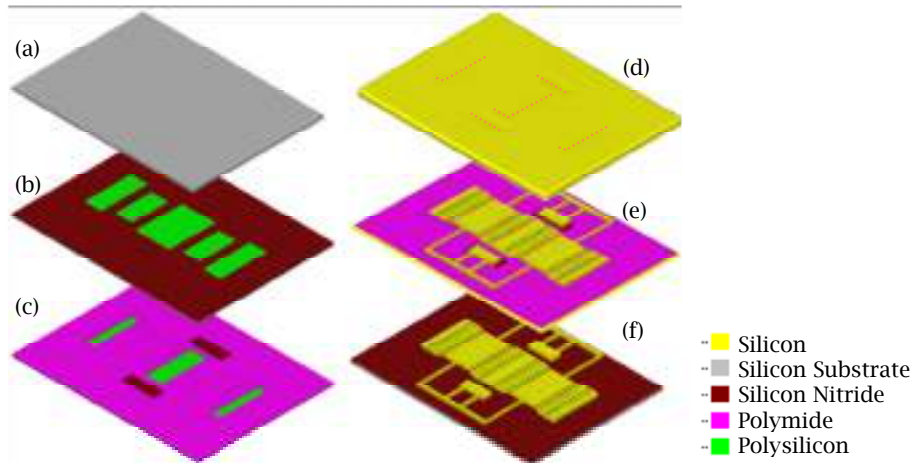

Fig. 3: Fabrication process modeling of the gyroscope.

4. DEVICE PERFORMANCE SIMULATION

4.1 Modal Analysis
Using the CAD geometry created from the process modeling, we perform the finite element analysis to extract the resonant frequencies and mode shapes from the MEMS gyroscope. The three key vibration responses related to the device's operation are obtained with CoventorWare and are shown in Fig. 4, where the displacements are exaggerated by ten times. Fig. 4(a) illustrates the vibration mode in the X direction for an in-plane gap closing motion between finger sidewalls. The resonant frequency for the X mode is found to be around 185.1 kHz. The driving mode for the in-plane vibration in the Y direction shown in Fig.4 (b) has a corresponding resonant frequency of 73.7 kHz. The sensing mode for the out-of-plane vibration in Z direction is shown in Fig.4 (c), which has a resonant frequency of 26.7 kHz. The large difference in resonant frequencies between the driving Y mode and the sensing Z mode implies the necessity of design change for performance improvement.

4.2 Frequency Response Analysis
To understand the device's frequency characteristics, we conduct the frequency response analysis by assembling a behavior model of the system using the Architect module in CoventorWare. The behavior model enables quick what-if analyses of the device under various mechanical and electrical stimuli. Solutions can be obtained with comparable accuracy to that of the finite element simulation, which requires a full-size problem to be solved at each frequency point. Fig. 5 shows the behavior model of the MEMS gyroscope with illustrations of the 3D physical geometry mapped to the corresponding behavior symbols.
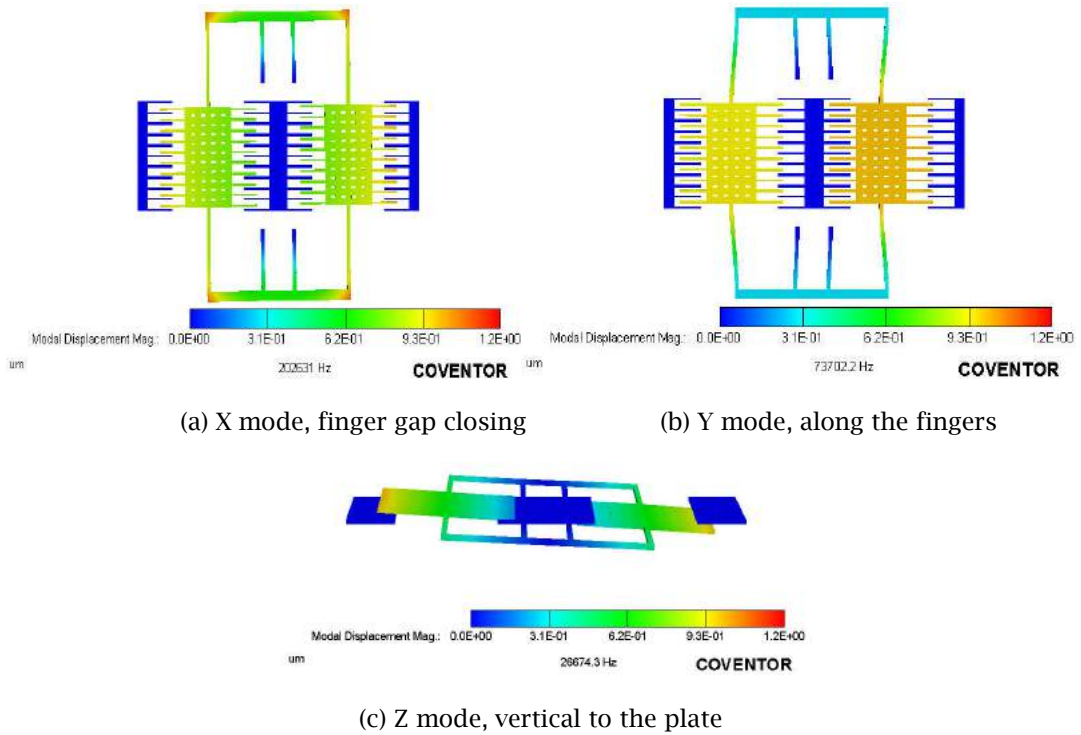
(a) X mode, finger gap closing

(b) Y mode, along the fingers

(c) Z mode, vertical to the plate

Fig. 4: The three major vibration mode shapes.

a. Anchor
b. Beam
c. L-beam
d. Proof mass and
   movable fingers
e. Electrodes underneath
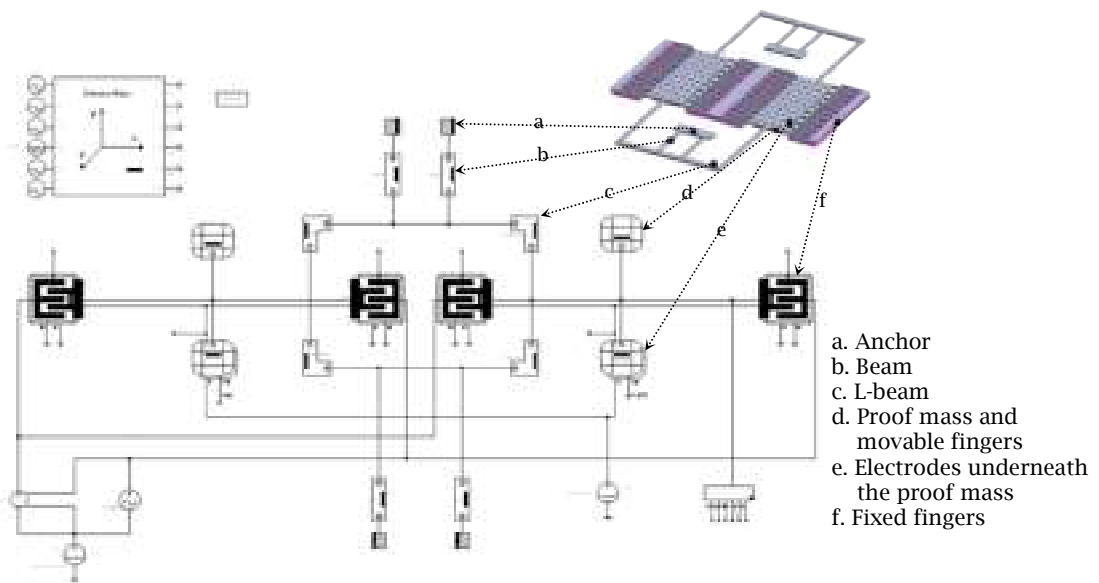   the proof mass
f. Fixed fingers

Fig. 5: Schematic design of the gyroscope.

The behavior symbols are selected from CoventorWare parametric component libraries for MEMS. Each symbol takes a few inputs such as size and position parameters based on the 3D design geometry.

They are connected with each other via knots to generate a system schematic diagram. The complicated mathematical descriptions for detailed physical models are reduced to a small number of degrees of freedom for the symbolic models in the schematic description. As a result, complex MEMS involving multiple physical domains and peripheral subsystems can be studied with ease at a high level of abstraction. As the highest resonant frequency among the three modes of interest here is less than 200 kHz, the analysis is performed in a frequency range from 0 to 200 kHz. The simulation is finished in less than 10 seconds. Fig. 6 shows the frequency response of the MEMS gyroscope.
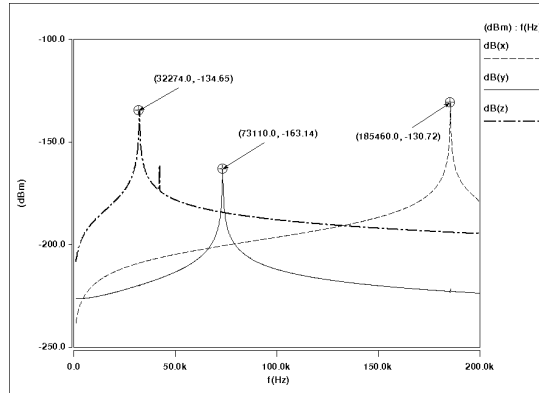

Fig. 6: Resonant frequency response of the gyroscope.

From Fig. 6, we observe that the frequency curves peak at 185.5 kHz for the X mode, 73.1 kHz for the Y mode and 32.3 kHz for the Z mode, respectively. This confirms that the driving Y mode and the sensing Z mode have a very weak correlation in the current design. To achieve optimum sensitivity, it is desirable that the two resonant frequencies be as close as possible. Therefore, adjusting some key design parameters and configurations is needed for design optimization.

4.3 Design Optimization

Since the resonant frequency is a function of the structural stiffness, adjusting the suspension beam dimensions can effectively change the beam stiffness hence the resonant frequency. Our first effort is to change the width of Beam 1, as shown in Fig. 2, to determine the optimum conditions. The frequency response of the structure with various beam widths is shown in Fig. 7. The width of the beam is adjusted from 8 to 24 μm with a 4 μm increment. The frequency responses for all three modes show the same tendency: wider beams have higher resonant frequencies. However, the resonant frequency shift ranges are different: the X mode has the largest shift and the Z mode has the smallest one. Decreased beam width leads to better coupling between Y and Z modes; but it also leads to a smaller resonant frequency of the X mode. As a result, the choice of the Beam 1 width is a tradeoff between the Y-Z mode correlation and the location of X mode resonant frequency.

The same optimization process is applied to the Beam 2. Fig. 8(a) shows the results. The beam width is adjusted from 4 to 20 μm with a 4 μm increment. The resonant frequencies of the structure in all three modes are dependent on the beam width: wider beams have higher resonant frequencies. In contrast to relatively small changes of the Z and X modes, the frequency change of the Y mode has a much wider range from 15 to 100 kHz. With a 4 μm beam width, the Y and Z modes have similar resonant frequencies and the X mode has a much higher one. However, the 4 μm feature size brings challenges to the device fabrication and material selection, which often lead to an increased cost. Therefore, adjusting beam width is proved to be beneficial in some aspects but deleterious in others.

The effect of the length of Beam 2 on the resonant frequencies of all three modes is shown in Fig. 8(b). The beam width is fixed at 4 μm and the length is adjusted from 250 to 400 μm. In general, long beams facilitate the deflection of the proof mass during the vibration. The simulation results indicate that the beam length influences the three modes in the same fashion: a longer beam reduces the resonant

frequencies of all three modes. The shift magnitudes for the Y and Z modes are higher than that for the X mode. In another word, as the beam becomes longer the undesired mode, X mode, is moved further away from the desired modes, Y and Z modes. Therefore, longer beams are preferred in our gyroscope design.
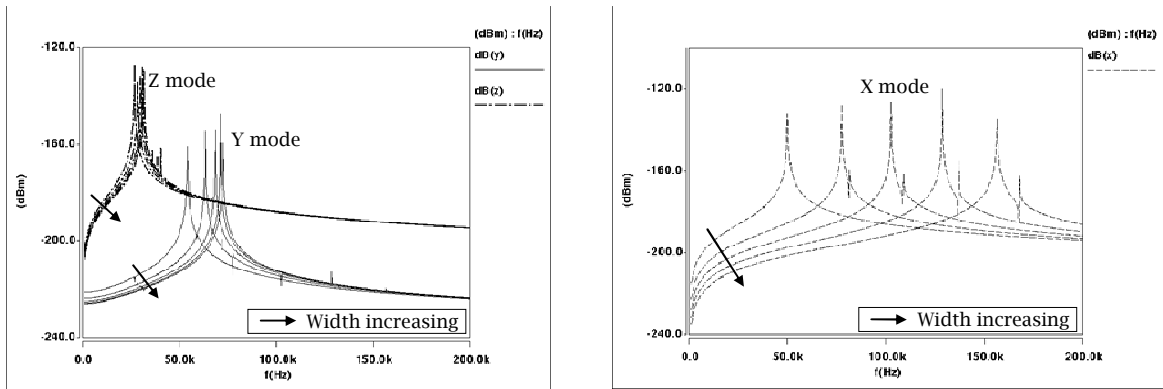
(a) Y and Z modes   (b) X mode

Fig. 7: Effect of Beam 1 width on the resonant frequencies.
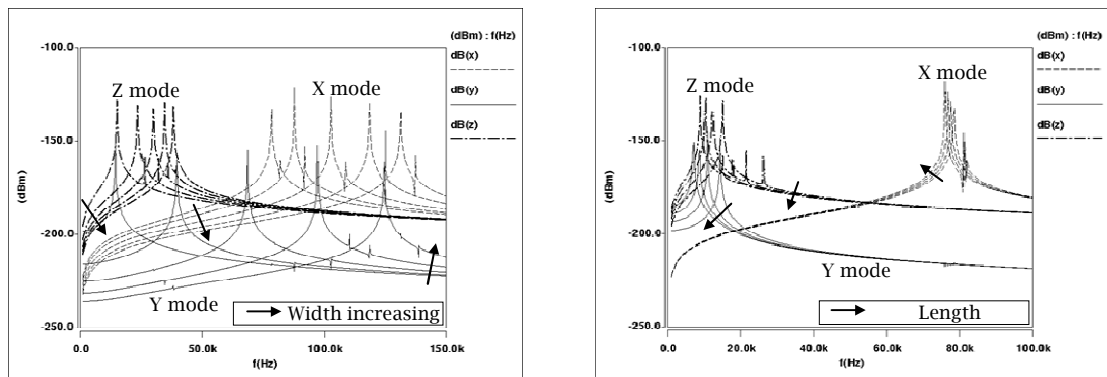
(a) Width effect   (b) Length effect

Fig. 8: Effect of Beam 2 dimensions on the resonant frequencies.

Combining the results from the initial optimization efforts, the desired geometry of the design can be obtained when Beam 1 is 16 μm by 450 μm and Beam 2 is 4 μm by 400 μm. Fig. 9 shows the device structure and its frequency response. The suspense beams have low stiffness and the resonant frequencies for the X, Y, and Z modes are 75.9, 7.1 and 8.9 kHz, respectively.

The results demonstrate a good coupling between the driving Y mode and the sensing Z mode. However, this optimized design is not suitable for device miniaturization. The device with the 400 μm long beam is difficult to fit in compact packages. The 4 μm features often require extra constraints and increase the cost of the fabrication process. Moreover, the performance of the device may be easily affected by the environmental factors such as deformation of the package and temperature drift.

In order to achieve both a low stiffness and miniaturization of the device, folded-beam design is incorporated. The folded beam model can be easily generated by inserting the highlighted components into the original design (Fig. 10). The design parameters are: Beam 1 is 20 μm by 450 μm, Beam 2 is 6

µm by 250 µm, the folded structure is 10 µm by 187.5 µm. The results show that the resonant frequencies of the X, Y, and Z modes are 77.3, 20.6, and 18.1 kHz, respectively.

(a) The optimized model   (b) The improved frequency response
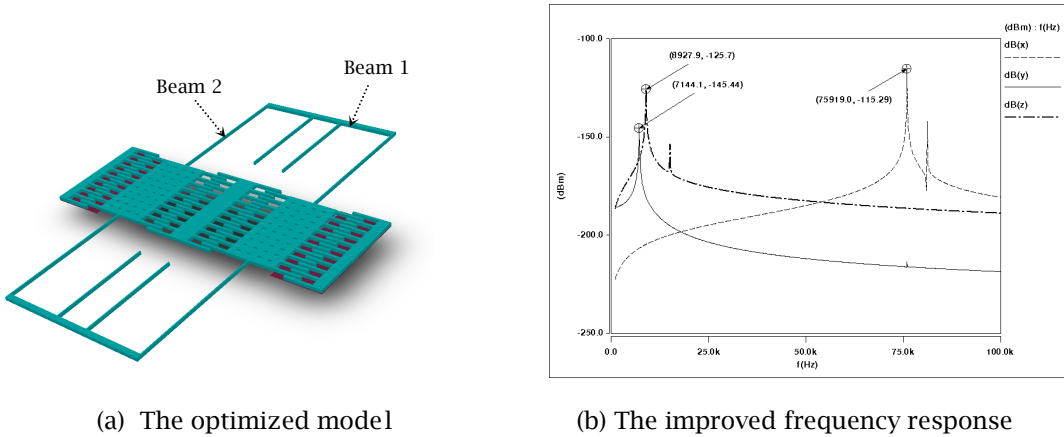
Fig. 9: Parameter optimization and the corresponding frequency response.
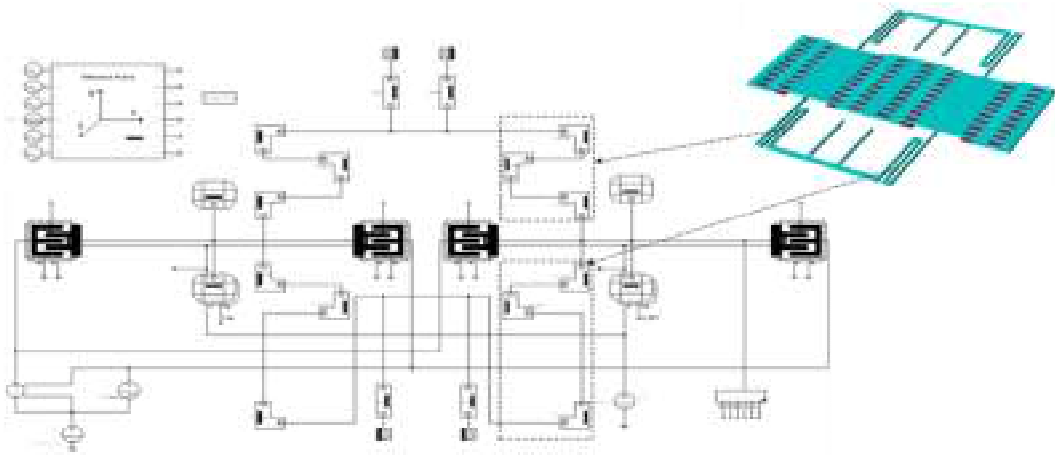

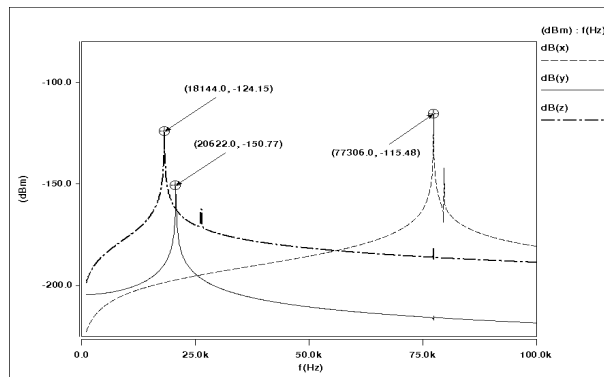Fig. 10: Schematic model of the folded-beam gyroscope.

Fig. 11: Frequency response of the optimized folded-beam design.

The folded-beam design demonstrates high performance, which is similar to the original long-beam design. It is also more compact and easier for miniaturization purposes. Furthermore, the smallest feature of the new design is 6 µm, 50% more than the initial design; this can greatly reduce the fabrication complexity and the cost of the final device.

4.4 Design Sensitivity and Monte Carlo Analysis

Geometry variations are inevitable in any microfabricated devices. A design sensitivity analysis is conducted to show how parameter perturbation affects the resonant frequency (20.6 kHz) of the driving Y mode for the folded-beam design. We choose four design parameters from the optimized structure, namely the width and length of Beam 1 and Beam 2. The design sensitivity, defined as the derivative of the resonant frequency with respect to the design parameter, is obtained with CoventorWare. Tab. 2 shows the impact of the parameter perturbation on the Y mode resonant frequency.

	Parameter	Sensitivity	Nominal size (µm)	Perturbation (µm)	Change in Frequency (Hz)
Beam 1	Width	0.019	16	0.2	4.89
	Length	-0.019	450	0.2	-0.19
Beam 2	Width	1.480	6	0.2	1016.3
	Length	-1.470	250	0.2	-24.2

Tab. 2: Influence of parameter perturbation on the Y mode resonant frequency (20.6 kHz).

A constant perturbation error of 0.2 µm is assumed for all design parameters, e.g., induced by tolerance in fabrication process. The perturbation is normalized to the nominal value for each parameter. For instance, the width of Beam 2 shows a 3.33% variation due to the perturbation. The width parameter has a sensitivity of 1.48. When multiplied by the normalized perturbation, the sensitivity yields the normalized change in the resonant frequency, i.e., $3.33\% \times 1.48 = 4.93\%$. In absolute terms, the frequency change due to the width variation can be calculated as $4.93\% \times 20.6$ kHz = 1016.3 Hz. The sensitivity analysis unveils the parameters that are most likely to cause frequency drift and performance deterioration, and can be used to guide design decisions early in the development cycle.

The MEMS gyroscope is next studied with Monte Carlo simulation to estimate the uncertainty in mass production due to random variation in design parameters. The four parameters listed in Tab. 2 are given a normal distribution around their nominal values. Monte Carlo analysis is carried out on the resonant frequency in the Y direction with 500 sample points. An acceptable driving frequency range is predefined as ±3% deviation from the nominal value of 20.6 kHz, i.e., between 20 kHz (lower bound) and 21.2 kHz (upper bound). Fig. 12 shows the simulated yield results. The top histogram in Fig. 12 shows the statistical distribution of the resonant frequency in Y direction due to the random variation in the design parameters. The bottom plot in Fig. 12 gives the measured frequency for each of the 500 sample points. The yield of the mass production is predicted to be 75%, which means 75% of the device samples out of the mass production will have a driving mode resonant frequency within the acceptable frequency range.

The Monte Carlo analysis reveals the uncertainty propagation, and estimates the yield impact of the design parameter variations. Information derived from the analysis can help bring insights into the fabrication process control to increase the yield of the mass production.

5. PACKAGE ANALYSIS

Gyroscopes do not require a physical contact with the outside world; the package can therefore be hermetically sealed. The package should have little or no influence on the sensor performance; it should not affect the frequency response of the sensor. Of concern here is how the packaged sensor performs in extreme operating conditions with a wide temperature range.
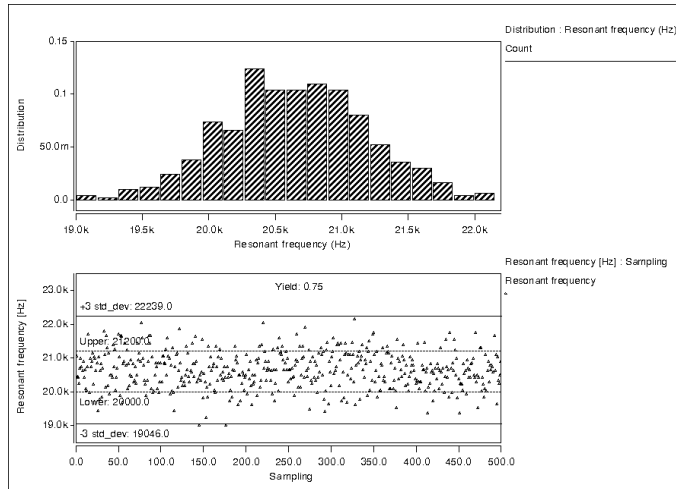
Fig. 12: Sensitivity analysis for Y mode frequency.

Given the small dimension of the designed folded-beam gyroscope, the sensor is packaged as a surface mounted device (SMD). A package model, SMD_KD_VA3703 from the ConventorWare package library, is selected. The lateral dimension of the package is 3.2×2.8 mm^2 and the cavity to contain the sensor is 942×842 μm^2. The gyroscope is mounted on the substrate of the cavity as shown in Fig. 13. The four pins are fixed on the printed circuit board, and are subject to the temperature loading ranging from -40 ˚C to 120 ˚C with an increment of 40 ˚C. The thermally induced mechanical stress is solved by the finite element method and is shown in Fig. 13.

(a) Top view   (b) Rear view

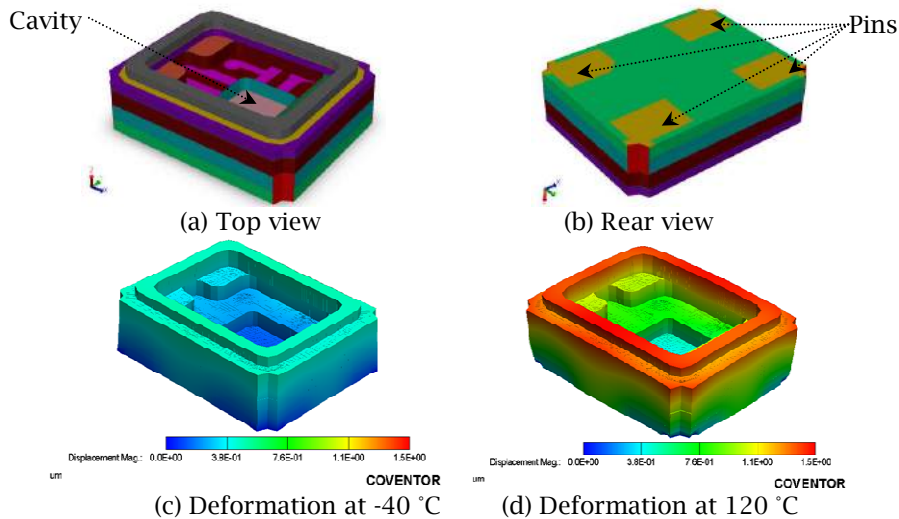(c) Deformation at -40 ˚C   (d) Deformation at 120 ˚C

Fig. 13: Package model and thermal-induced deformation.

The finite element analysis provides the temperature distribution and mechanical deformation of the package. The information can be imported to the system-level modeling to estimate the real-time sensitivity of the gyroscope. The frequency responses of the device at the four different operating temperatures are shown in Fig. 14. We can see that the resonant frequency decreases as the operating temperature increases. The frequency shift is relatively small though, with a difference less than 100

Hz in the given temperature range. Compared to the fabrication uncertainties, the effect of the temperature-induced package deformation on the resonant frequency is nearly negligible.

6. CONCLUSIONS
This paper describes an integrated simulation workflow that incorporates the modeling of fabrication process, device design and packaging through a case study of a MEMS tuning-fork gyroscope using CoventorWare. A MEMS gyroscope design is generated based on mask layout and fabrication process restrictions, and analyzed using finite element and behavior modeling approaches. To increase the driving and the sensing mode correlation for the sensor, the design is optimized through parameter sweeping and configuration modification. A folded-beam design with tailored parameters is proposed to achieve both a low stiffness and compactness for the miniaturized device. Design sensitivity analysis suggests that the device performance is highly sensitive to the suspension beam width. A fabrication-induced variation of 0.2 μm in a beam width can lead to a driving mode frequency shift of over 1000 Hz. With a small sample Monte Carlo analysis, the yield of gyroscope mass production is estimated to be 75%, provided that the acceptable range for the driving frequency is within ±3% deviation from its nominal value. Thermal stress analysis of a SMD package is also performed to model the packaged sensor undergoing extreme temperature variations. Results show that the maximum temperature-induced frequency shift in the MEMS device is less than 100 Hz in a temperature range from -40 ˚C to 120 ˚C. The integrated multi-level simulation presented in this paper demonstrates to be an effective way of optimizing the MEMS device to significantly reduce post-design fabrication cost and improve device performance.
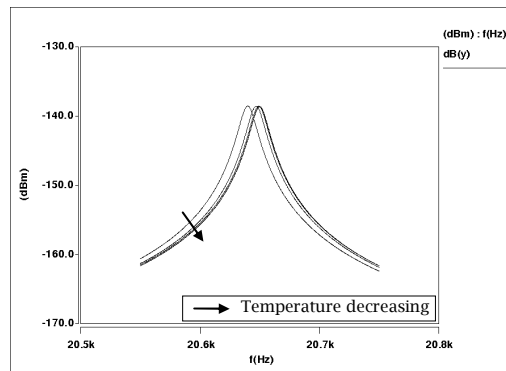

Fig. 14: Resonance frequencies of the device at various temperatures.

7. ACKNOWLEDGEMENTS

8. REFERENCES
[1]   Elwenspoek, E.; Wiegerink, R.: Mechanical Microsensors, Springer, Germany, 2001.
[2]   Bryzek, J. et al: Marvelous MEMS, Circuits and Devices Magazine, IEEE, 2006.
[3]   Yazdi, N. et al: Micromachined inertial sensors, Proceedings of the IEEE, 86(8), 1998, 1640-1659.
[4]   Maenaka, K.; Shiozawa, T.: A study of silicon angular rate sensors using anisotropic etching technology, Sensors and Actuators A Physical, 43, 1994, 72-77.
[5]   Maenaka, K. et al: Analysis of a highly sensitive silicon gyroscope with cantilever beam as vibrating mass, Sensors and Actuators A Physical, 54, 1996, 568–573.
[6]   Putty, M.; Najafi, K.: A micromachined vibrating ring gyroscope, International Conference on Solid-State Sensor and Actuator Workshop, Hilton Head Island, SC, 1994, 213–220.
[7]   Hashimoto, M. et al: Silicon resonant angular rate sensor using electromagnetic excitation and capacitive detection, Journal of Micromechanics and Microengineering, 5(3), 1995, 219–225.

[8] Voss, R. et al: Silicon angular rate sensor for automotive applications with piezoelectric drive and piezoresistive read-out, International Conference on Solid-State Sensors and Actuators, Chicago, IL, 1997, 879–882.

[9] Bernstein, J. et al: A micromachined comb-drive tuning fork rate gyroscope, Journal of Microelectromechanical Systems, 1993, 143-148.

[10] Soderkvist, J.: Micromachined gyroscopes, Sensors Actuators A, 43, 1994, 65–71.

[11] Moussa, H.; Bourquin, R.: Theory of direct frequency output vibrating gyroscopes, IEEE Sensors Journal, 6(2), 2006, 310-315.

[12] Acar, C.; Shkel, A. M.: Nonresonant micromachined gyroscopes with structural mode-decoupling, IEEE Sensors Journal, 3(4), 2003, 487-506.

[13] Acar, C.; Shkel, A. M.: Structural design and experimental characterization of torsional micromachined gyroscopes with non-resonant drive mode, Journal of micromechanics and Mircoengineering, 14, 2004, 15-25.

[14] Gyimesi, M. et al: Finite-element simulation of micro-electromechanical systems (MEMS) by strongly coupled electromechanical transducers, IEEE Transactions on Magnetics, 40(2), 2004, 557-560.

[15] Zhang, C. et al: 3D MEMS design method via Solidworks, Proceedings of 1st IEEE International Conference on Nano/Micro Engineering and Molecular Systems, 2006, 747-751.